Biphasic release of the alarmin HMGB1 early after trauma predicts poor clinical outcome

William Ottestad, MD[1,2]; Ingrid N. Rognes, MD[2]; Soeren E. Pischke, MD PhD[1,3];
Tom E. Mollnes, MD PhD[3,4,5]; Ulf Andersson, MD PhD[6]; and Torsten Eken, MD PhD[1,2]

[1] Department of Anaesthesiology, Oslo University Hospital, Oslo, Norway

[2] Institute of Clinical Medicine, Faculty of Medicine, University of Oslo, Oslo, Norway

[3] Department of Immunology, Oslo University Hospital, and K.G. Jebsen IRC, University of Oslo, Norway

[4] Research Laboratory, Nordland Hospital, Bodø, and Faculty of Health Sciences, K.G. Jebsen TREC, University of Tromsø, Norway

[5] Centre of Molecular Inflammation Research, Norwegian University of Science and Technology, Trondheim, Norway

[6] Department of Women's and Children's Health, Karolinska Institutet, Karolinska University Hospital, Stockholm, Sweden

Correspondence to:

Torsten Eken
Department of Anaesthesiology
Oslo University Hospital
PO Box 4956 Nydalen
NO-0424 Oslo
Norway

E-mail: torsten.eken@medisin.uio.no

Phone: +47 950 79 939
Fax: +47 221 19 857

Reprints will not be ordered.

Conflicts of Interest and Source of Funding:

All authors have declared that no conflict of interest exists.

This study was financially supported by Oslo University Hospital, the University of Oslo, South-Eastern Norway Regional Health Authority, the Karolinska Institutet, The Research Council of Norway, The Norwegian Council on Cardiovascular Disease, and the European Community's Seventh Framework Programme under grant agreement n° 602699 (DIREKT).

Word count: 3,029 total (references not included), including abstract 236 words

Abstract

Objective: The causal role of the prototype alarmin high mobility group box 1 protein (HMGB1) in systemic inflammation and remote organ injury after trauma and shock is established in animal models but not in humans. Our aim was therefore to determine HMGB1 concentration kinetics with high time resolution during the first hours after trauma in individual patients, and investigate the association with outcome.

Design: Prospective single-center observational study.

Setting: University hospital Level I trauma center.

Patients: Convenience recruitment of 136 trauma patients.

Interventions: None.

Measurements and Main Results: Total plasma HMGB1 levels were analyzed with ELISA in repeated samples. Relationships between predefined predictor variables and outcome were examined in multivariable linear regression models. Ventilator-free days was used as primary outcome measure. Two distinct HMGB1 release phases were identified. An initial exponential decay phase with half-life 26 min was not correlated with outcome. In contrast, a second HMGB1 wave peaking 3-6 hours after trauma in the most severely injured and physiologically deranged patients was consistently the most important predictor of outcome in our multivariable models, rendering all other predictor variables insignificant except for smaller contributions from age and sex, and of admission base excess for maximal creatinine concentration.

Conclusions: HMGB1 was released in two consecutive phases. Only the second HMGB1 wave was a significant predictor of outcome. Patients with a high HMGB1 concentration between 3 and 6 hours after trauma might hypothetically benefit from HMGB1-specific antagonist therapy.

Key Words: wounds and injuries; systemic inflammatory response syndrome; multiple organ failure; alarmins; HMGB1 protein; prognosis

Introduction

Severe trauma may be lethal even if patients survive initial treatment. Ruptured, leaky or injured cells release preformed endogenous danger signals, called alarmins or damage-associated molecular pattern molecules (DAMPs), which activate the innate immune system (1, 2). An overwhelming systemic inflammatory response may ensue, with remote organ injury and predisposition to invasive infections (3). Causal therapy is still lacking.

The prototypical alarmin high mobility group box 1 protein (HMGB1) is an evolutionary ancient DNA-binding protein present in all eukaryotic cells and in platelets (2, 4-7). In the nucleus, HMGB1 organizes DNA and nucleosomes and regulates gene transcription. HMGB1 is passively released from dying cells, or actively secreted from stressed or activated cells (5). Extracellular HMGB1 serves as a powerful mediator of inflammation, directing chemokine, cytokine, neuroimmune, or metabolic activities (2, 8-12). Its two dominant receptors are toll-like receptor 4 (TLR4) (5, 8, 9) and receptor for advanced glycation end products (RAGE) (10, 13).

Human and rodent HMGB1 have 99% protein sequence identity (4), strengthening the translational value of experimental models. Experimental work in rodents has established a central role for HMGB1 in systemic inflammation and remote organ injury after trauma, and administration of HMGB1 antagonists has proven beneficial (14-18). Trauma with hemorrhagic shock causes acute lung injury (ALI) via release of HMGB1 from gut epithelial cells, and mice selectively lacking HMGB1 in these cells are protected from developing ALI after trauma (18), as are TLR4 mutant mice (18, 19). Hemorrhagic shock-induced HMGB1 release also initiates RAGE-mediated endocytosis of HMGB1 in lung vascular endothelial cells (9), contributing to ALI.

HMGB1 antagonist-based therapy has not yet been studied clinically, and observational studies of quantitative and temporal aspects of HMGB1 release in trauma patients have yielded somewhat diverging results (20-23). We have therefore examined relationships between injury, plasma HMGB1 concentration kinetics, and outcome in detail in individual trauma patients with a broad range of injury severities, adjusting for confounders. Our hypothesis was that HMGB1 concentration as a function of time during the first hours after injury could predict outcome and provide a starting point for design of clinical studies with HMGB1 antagonists, in particular regarding time of therapeutic intervention.

Materials and Methods

Study Design and Approval

This prospective observational study relied on convenience recruitment of trauma patients admitted January 2011 through January 2014 to Oslo University Hospital (OUH) Ullevål, a Norwegian Level I trauma center. A wide spectrum of injuries and physiological derangements was strived for. All patients ≥18 years who met criteria for trauma team activation were eligible for enrollment. Patients with burn injuries and pregnant women were not included. Patients were followed until ten days, discharge from intensive care unit (ICU), or death, whichever came first. Reference HMGB1 values were obtained from 20 healthy volunteers.

We adhered to the STROBE statement for cohort studies (24). All parts of the study were approved by the Regional committee for medical and health research ethics (2010/2014 REK Sør-Øst D), in accordance with the Declaration of Helsinki. Patients were enrolled on admission, and written informed consent was obtained as soon as practically possible. A temporary written consent from the closest relative was obtained when patients were unable to consent. All material was destroyed if patients or relatives did not consent.

The Regional committee for medical and health research ethics approved the use of biological material from patients who died before consent could be obtained, and the use of written information with the possibility for withdrawal for patients who were transferred to other hospitals or discharged before consent could be obtained. All those patients were checked against the Norwegian national biological research reservation registry before final inclusion.

Sample Collection and Analyses

Blood was drawn in K_2EDTA coated tubes (Vacuette 454209, Greiner Bio-One International GmbH, Austria) immediately after admission, 2, 4, 6, and 8 h thereafter, and every morning in the ICU. Five patients had additional samples drawn during helicopter transfer. All sampling times were converted to elapsed time from injury.

Sampling through an arterial cannula was preferred in order to obtain blood that was not draining from any particular injured body part. Samples were drawn from a central venous line or from a peripheral vein if an arterial line was not present. Peripheral venous samples from healthy volunteers were handled according to the same protocol. The EDTA tubes were put directly in ice slush after 8-10 inversions, and within 15 min centrifuged at 2500 g for 15 min at 4 °C. The supernatant was immediately transferred to sterile polypropylene tubes (NUNC CryoTubes; Thermo Fisher Scientific, Waltham, MA) and stored at −80 °C. Samples obtained during helicopter transfer were stored in an insulated bag with ice packs until admission.

Plasma HMGB1 concentrations were determined with ELISA (HMGB1 ELISA Kit II, Shino-Test Corporation, Japan). Material from 12 pilot patients was analyzed separately, all other samples were analyzed in one batch. Values below the lower detection limit (LDL, 0.313 ng/mL) were set to LDL. Single sample analyses were deemed sufficient due to low intra-assay variability (25). All concentration measurements were conducted blinded to clinical information.

Clinical Data

Clinical data were defined according to The Utstein trauma template (26) and collected from the OUH Trauma Registry. Anatomic injury was coded according to the Abbreviated Injury Scale (AIS) 1990 Revision Update 98 (27). New Injury Severity Score (NISS) was chosen as a measure of overall injury severity (28, 29) and admission base excess (BE) as a measure of physiological derangement (30). Patients transferred to ICUs in other hospitals while still intubated were regarded as ventilator treated through the rest of the 30-day period. Patients transferred to hospitals abroad before 30 days were regarded as alive at 30 days.

All outcome measures and predictor variables were predefined. Primary outcome measure was days alive and off ventilator during the first 30 days after trauma (ventilator-free days, VFD) (31, 32). Lung dysfunction is the most frequent organ failure after trauma (33), and VFD is considered a combined measure of mortality and duration of ventilation (32). Mortality was not included as endpoint, as deaths were anticipated to be few and mainly due to head injuries (34). Secondary outcome measures, focusing on early signs of remote organ injury (35), were maximal serum creatinine, alanine aminotransferase (ALT), aspartate aminotransferase (AST), and bilirubin within 48 h after injury, and body weight-adjusted total noradrenaline dose administered from 8 h through the 24-h period starting no later than 48 h after admission. Predictor variables were sex, age, mechanism of injury (blunt or penetrating), NISS, BE, admission HMGB1 concentration, and area under the individual HMGB1 concentration curves (AUC) (36) (Supplemental Methods, Supplemental Digital Content 1).

Patients with severe head trauma spend substantial time on ventilator support due to the head injury per se, their noradrenaline dose being guided by cerebral perfusion pressure. Patients with maximal AIS severity code ≥3 in Injury Severity Score region Head or neck were therefore excluded from analyses of VFD and accumulated noradrenaline dose. Similarly, all patients with an AIS code in region Abdominal or pelvic contents were excluded from analyses of ALT, AST and bilirubin.

Statistics

Data analysis was undertaken using JMP 11.2.1 and 13.1.0 (SAS Institute, Cary, NC). Correlation between continuous variables was assessed with the Spearman correlation coefficient (ρ) and linear regression as appropriate,

and categorical data were compared using Fischer's Exact test. A two-tailed $p \leq 0.05$ was chosen to represent statistical significance.

Relationships between predictor and response variables were further examined in multivariable linear regression analyses with backward elimination. Significance levels were set to 0.05 for entry into and 0.10 for elimination from the model. Robustness of results was tested by removing individuals having residuals outside or equal to the 1 and 99 percentile and rerunning the analysis, and log-transforming where evidence of skewed residuals was found (not shown). Results changed only marginally.

Assessment of importance of the individual predictor variables in multivariable models was performed as variance-based sensitivity analysis. Importance indices were constructed from observed combinations of factor values, since predictor variables were generally correlated.

Results

Population and Outcome

A total of 145 patients were enrolled. Two withdrew consent, one was <18 years, three were included in an interventional study, and three had unknown time of injury (Supplemental Digital Content 2). Characteristics of the remaining 136 patients constituting the study population are given in Table 1 and Supplemental Table 1 (Supplemental Digital Content 3).

Samples from 1094 time points were analyzed; 969 were arterial, 17 central venous, 105 peripheral venous, and three undocumented. Median time from injury to first sample was 75 min (quartiles 47-110). Median HMGB1 concentration in venous samples from healthy subjects was 0.69 ng/mL (0.58-0.88) (Table 1).

HMGB1 Concentration on Admission

Bivariable associations between admission HMGB1 concentration, patient age and sex, injury, and outcome are shown in Supplemental Tables 2 and 3 (Supplemental Digital Content 3). Admission HMGB1 concentration rose with increasing NISS and decreasing BE, was higher in blunt injuries, and was correlated with all outcome measures except maximal bilirubin concentration. All outcome measures were correlated with NISS, and most with BE.

In contrast, admission HMGB1 concentration was not a significant predictor for any outcome measure in multivariable analyses, except for a weak contribution to maximal ALT and AST (Supplemental Table 4, Supplemental Digital Content 3). Thus, most observed associations between admission HMGB1 and outcome were caused by confounding factors not accounted for in bivariable analyses.

HMGB1 Concentration as a Function of Time

Relationships between area under the individual HMGB1 concentration curves (AUC) and outcome measures were explored in detail, since the impact of HMGB1 on the immune system was presumed to be a function not only of admission concentration but also of concentration over time.

Fig. 1 shows HMGB1 concentrations as a function of time after injury for all included patients. The profiles were strikingly similar: An immediate phase when concentrations fell rapidly, followed in some patients by a “shoulder” with a slower concentration decline subsiding within approximately 6 h in most patients. Later HMGB1 concentrations were generally low. No patient had HMGB1 values >12 ng/mL from 48 h after injury and through their ICU stay.

We endeavored to separate the immediate phase from the "shoulder" in individual patients. HMGB1 concentration decay rates from the first to the second in-hospital samples were directly proportional to admission concentrations (Fig. 1), i.e., the concentrations followed a first order elimination kinetic in the immediate phase after injury. The decay rate was 0.40 h^{-1} for the 126 sample pairs constituting the total population (95%CI 0.38-0.42; R^2=0.92; p<0.0001); removing the single highest admission value and restricting analysis to patients arriving within one hour after injury yielded nearly identical results (48 pairs; decay rate 0.41 h^{-1}, 95%CI 0.40-0.43; R^2=0.99; p<0.0001). An exponential decay curve could therefore be fitted to the measured concentrations (70 sample pairs; see Supplemental Methods, Supplemental Digital Content 1). The estimated elimination rate constant k (1.613 h^{-1}, corresponding to a half-life of 26 min) was utilized to decompose all individual measured HMGB1 concentration curves into a computed immediate exponential decay curve and a residual curve, defined as the difference between the measured concentrations and the computed decay curve (Fig. 2). Admission HMGB1 concentrations increased with anatomical injury, while residual curves were more prominent in patients who were also physiologically deranged (Fig. 3).

Total area under an exponential decay curve is proportional to the initial concentration. Consequently, as for admission HMGB1, AUC for the exponential decay curve was not a significant predictor for any outcome measures in multivariable models, except for a weak contribution to maximal ALT and AST. We therefore presumed that any relationship between HMGB1 concentration and outcome would reside in the residual curves. The "shoulders" blunting the initial rapid decay in many of the measured concentration curves (Figs. 1-3) were visible as prominent "second waves" at 3-6 h in the residual curves (Fig. 2; lower rows in Fig. 3), increasing in size both with injury severity and physiological derangement. Quantitative relationships were therefore investigated using AUC from 3 to 6 h after injury (second wave $AUC_{3\text{-}6}$) as a continuous variable.

In bivariable analyses (Supplemental Tables 2 and 3, Supplemental Digital Content 3), second wave $AUC_{3\text{-}6}$ was significantly correlated with admission HMGB1, NISS, and BE after blunt injury, and with all outcome measures. In multivariable analyses (Table 2), both NISS and admission HMGB1 were rendered insignificant as predictors of outcome, and BE only contributed to maximal creatinine. Second wave $AUC_{3\text{-}6}$ was consistently the most important outcome predictor, alone explaining 62% of the variability in noradrenaline usage in patients without major head injury, and explaining 88% of VFD variability with a smaller contribution from age. It was also the most important contributor to ALT and AST in patients without abdominal injuries. Second wave $AUC_{3\text{-}6}$ was itself predicted by admission HMGB1 and BE.

Discussion

Trauma represents extreme stress at the cellular level. Transcriptional evidence documents an early global reprioritization of the leukocyte transcriptome, affecting a majority of cellular functions and pathways (37). Further, up to 70% of plasma proteins from trauma patients originate from intracellular components (38). One might thus expect to find significant positive or negative correlations between almost any set of molecules and outcome. Multivariable analyses are therefore necessary to explore the relative importance of putative outcome predictors. In line with this, we confirmed previous reports that admission HMGB1 concentration was significantly correlated with NISS, BE, VFD, and markers of organ injury in bivariable analyses (21), whereas multivariable analyses left admission HMGB1 only as a weak explanatory variable for maximal ALT and AST, and only if second-wave HMGB1 was not in the model.

The immediate release of HMGB1 primarily reflected the anatomical extent of the injury (Table 2; cf. Fig. 3), reconcilable with passive release due to tissue necrosis which is expected to generate a redox isoform that primarily promotes chemotaxis (39). In contrast, the second wave of HMGB1 release was a remarkably strong predictor of outcome. NISS and BE are robust predictors of outcome in trauma (30, 40), as confirmed in our analyses, however apart from a contribution of BE to maximal creatinine their predictive power was lost when the second wave was included in our multivariable model. The second wave was itself to a large extent predicted by admission BE and HMGB1. It is thus tempting to speculate that HMGB1 in the second wave acted as mediator of the combined detrimental effects of anatomical injury and physiological derangement after trauma. The biology behind its release is a matter of speculation, but experimental ischemia/reperfusion injury in the liver has been shown to induce active discharge of proinflammatory HMGB1 from hepatocytes within one hour of hypoxia (41). Regardless of cellular mechanism, based on the strong predictive value of BE we propose hypoperfusion with concomitant hypoxia and cellular stress as a likely cause for the second-wave HMGB1 (42).

The HMGB1 release kinetics in our trauma patients is in contrast to results from studies in sepsis, where serum levels increase gradually over the first 48 h and persist for a long period, making HMGB1 an exceptionally late mediator (43, 44). Instead, the biphasic pattern after trauma closely parallels that in acetaminophen-induced liver injury, a highly HMGB1-dependent condition studied extensively in both patients and animals (45). The initial hepatotoxic injury induces hepatocyte necrosis with HMGB1 release, causing leukocyte influx in the liver with subsequent generation of a second wave of HMGB1 that may be lethal due to TLR4/RAGE-mediated fulminant inflammation (46-48). Treatment with HMGB1-specific antagonists in acetaminophen-overdosed mice is highly successful and provides an extended therapeutic time window compared to standard therapy (8). We propose that the delayed treatment regimen in this cytotoxic model may have a direct translational value to trauma patients. It is tempting to speculate that it may be particularly important to antagonize the second wave of HMGB1, based on its strong association with outcome. This

would narrow the therapeutic time window down to the first few hours after trauma (Fig. 3), which is strikingly consistent with the observed time window anti-HMGB1 antibody therapy after experimental traumatic brain injury in rodents (49), which was efficacious up to 3 h but not at 6 h after trauma.

Limitations

The study has a relatively small size; however it is comparable to previous publications on HMGB1 in humans (21, 23). The short half-life of HMGB1 after injury has large effects on admission concentration due to varying prehospital times; the lack of a significant contribution of initial HMGB1 concentration to outcome in our multivariable analyses therefore does not necessarily imply lack of biological effect. The relationship between $AUC_{3\text{-}6}$ and therapeutic interventions, e.g., surgical procedures and blood transfusions, could not be explored in our material. Analyses regarding mechanism of injury are uncertain due to the low number of penetrating injuries. NISS was used as a summary measure of anatomical injury, but it lacks a direct relationship to the total volume of damaged tissue (29). The relationship between NISS and subsequent immunological activation is therefore complex.

Conclusions

The second wave of systemic HMGB1 release after severe trauma is a consistent predictor of forthcoming critical systemic inflammation. Its concentration time course may hypothetically point to a clinically accessible time window for future therapies blocking the detrimental effects of HMGB1 after trauma (17, 50).

Acknowledgments

We thank Signe Søvik for discussions and advice throughout the project, and Julie Katrine Lindstad for help with project design and ELISA analyses. We are grateful to Ivan Jonassen Rimstad, Astrid Arnesen Hug, Linda Soilammi, Erlend Skaga, and Tomas Drægni for help with recruitment of patients and acquisition of samples, and to Anne-Marie Siebke Trøseid, and Jens Petter Berg for help with optimization of pre-analytical conditions and for lab facilities. We are also grateful to the Department of Medical Biochemistry at Oslo University Hospital for providing routine lab analyses, and to Ronny Kristiansen for extracting them in electronic form. We thank the Oslo University Hospital Trauma Registry and registrars Morten Hestnes and Hans Johansson for providing clinical data, and the helicopter crews at the OUH Division of Pre-Hospital Services for their help in acquisition of prehospital samples. Ulf Kongsgaard is acknowledged for his support for the project from its inception.

Author contributions

TE conceived the study and was responsible for overall design; SP and TEM contributed to study design. WO, INR, and TE collected the data. INR performed the ELISA analyses with support from SP and TEM. TE and WO designed the statistical analyses and did the initial data interpretation; WO, INR, UA, and TE finalized analyses and interpretation. WO, UA, and TE wrote the first version of the manuscript, and all authors critically revised and approved the final version.

References

1. Asehnoune K, Hotchkiss RS, Monneret G: Understanding why clinicians should care about danger-associated molecular patterns. *Intensive Care Med* 2016; 42:611–614

2. Bertheloot D, Latz E: HMGB1, IL-1α, IL-33 and S100 proteins: dual-function alarmins. *Cell Mol Immunol* 2017; 14:43–64

3. Lord JM, Midwinter MJ, Chen Y-F, et al.: The systemic immune response to trauma: an overview of pathophysiology and treatment. *Lancet* 2014; 384:1455–1465

4. Kang R, Chen R, Zhang Q, et al.: HMGB1 in health and disease. *Mol Aspects Med* 2014; 40:1–116

5. Andersson U, Yang H, Harris HE: Extracellular HMGB1 as a therapeutic target in inflammatory diseases. *Expert Opin Ther Targets* 2018; 22:1–15

6. Vogel S, Bodenstein R, Chen Q, et al.: Platelet-derived HMGB1 is a critical mediator of thrombosis. *J Clin Invest* 2015; 125:4638–4654

7. Tsung A, Tohme S, Billiar TR: High-mobility group box-1 in sterile inflammation. *J Intern Med* 2014; 276:425–443

8. Yang H, Wang H, Ju Z, et al.: MD-2 is required for disulfide HMGB1-dependent TLR4 signaling. *J Exp Med* 2015; 212:5–14

9. Yang J, Zhao Y, Zhang P, et al.: Hemorrhagic shock primes for lung vascular endothelial cell pyroptosis: role in pulmonary inflammation following LPS. *Cell Death Dis* 2016; 7:e2363

10. Tian J, Avalos AM, Mao S-Y, et al.: Toll-like receptor 9-dependent activation by DNA-containing immune complexes is mediated by HMGB1 and RAGE. *Nat Immunol* 2007; 8:487–496

11. Xu J, Jiang Y, Wang J, et al.: Macrophage endocytosis of high-mobility group box 1 triggers pyroptosis. *Cell Death Differ* 2014; 21:1229–1239

12. Deng M, Tang Y, Li W, et al.: The Endotoxin Delivery Protein HMGB1 Mediates Caspase-11-Dependent Lethality in Sepsis. *Immunity* 2018; 49:740–753.e7

13. Rauvala H, Rouhiainen A: RAGE as a receptor of HMGB1 (Amphoterin): roles in health and disease. *Curr Mol Med* 2007; 7:725–734

14. Kim JY, Park JS, Strassheim D, et al.: HMGB1 contributes to the development of acute lung injury after hemorrhage. *Am J Physiol Lung Cell Mol Physiol* 2005; 288:L958–65

15. Yang R, Harada T, Mollen KP, et al.: Anti-HMGB1 neutralizing antibody ameliorates gut barrier dysfunction and improves survival after hemorrhagic shock. *Mol Med* 2006; 12:105–114

16. Levy RM, Mollen KP, Prince JM, et al.: Systemic inflammation and remote organ injury following trauma require HMGB1. *Am J Physiol Regul Integr Comp Physiol* 2007; 293:R1538–44

17. Shimazaki J, Matsumoto N, Ogura H, et al.: Systemic involvement of high-mobility group box 1 protein and therapeutic effect of anti-high-mobility group box 1 protein antibody in a rat model of crush injury. *Shock* 2012; 37:634–638

18. Sodhi CP, Jia H, Yamaguchi Y, et al.: Intestinal epithelial TLR-4 activation is required for the development of acute lung injury after trauma/hemorrhagic shock via the release of HMGB1 from the gut. *J Immunol* 2015; 194:4931–4939

19. Reino DC, Palange D, Feketeova E, et al.: Activation of toll-like receptor 4 is necessary for trauma hemorrhagic shock-induced gut injury and polymorphonuclear neutrophil priming. *Shock* 2012; 38:107–114

20. Peltz ED, Moore EE, Eckels PC, et al.: HMGB1 is markedly elevated within 6 hours of mechanical trauma in humans. *Shock* 2009; 32:17–22

21. Cohen MJ, Brohi KH, Calfee CS, et al.: Early release of high mobility group box nuclear protein 1 after severe trauma in humans: role of injury severity and tissue hypoperfusion. *Crit Care* 2009; 13:R174

22. Giannoudis PV, Mallina R, Harwood P, et al.: Pattern of release and relationship between HMGB-1 and IL-6 following blunt trauma. *Injury* 2010; 41:1323–1327

23. Namas RA, Vodovotz Y, Almahmoud K, et al.: Temporal patterns of circulating inflammation biomarker networks differentiate susceptibility to nosocomial infection following blunt trauma in humans. *Ann Surg* 2016; 263:191–198

24. Elm von E, Altman DG, Egger M, et al.: The Strengthening the Reporting of Observational Studies in Epidemiology (STROBE) statement: guidelines for reporting observational studies. *Lancet* 2007; 370:1453–1457

25. Lehner J, Wittwer C, Fersching D, et al.: Methodological and preanalytical evaluation of an HMGB1 immunoassay. *Anticancer Res* 2012; 32:2059–2062

26. Ringdal KG, Coats TJ, Lefering R, et al.: The Utstein template for uniform reporting of data following major trauma: a joint revision by SCANTEM, TARN, DGU-TR and RITG. *Scand J Trauma Resusc Emerg Med* 2008; 16:7

27. Association for the Advancement of Automotive Medicine: The Abbreviated Inury Scale 1990 Revision – Update 98. Des Plains, IL: Association for the Advancement of Automotive Medicine; 1998.

28. Osler T, Baker SP, Long W: A modification of the injury severity score that both improves accuracy and simplifies scoring. *J Trauma* 1997; 43:922–925

29. Balogh Z, Offner PJ, Moore EE, et al.: NISS predicts postinjury multiple organ failure better than the ISS. *J Trauma* 2000; 48:624–627

30. Ouellet J-F, Roberts DJ, Tiruta C, et al.: Admission base deficit and lactate levels in Canadian patients with blunt trauma: are they useful markers of mortality? *J Trauma Acute Care Surg* 2012; 72:1532–1535

31. Bernard GR, Wheeler AP, Arons MM, et al.: A trial of antioxidants N-acetylcysteine and procysteine in ARDS. The Antioxidant in ARDS Study Group. *Chest* 1997; 112:164–172

32. Schoenfeld DA, Bernard GR, ARDS Network: Statistical evaluation of ventilator-free days as an efficacy measure in clinical trials of treatments for acute respiratory distress syndrome. *Crit Care Med* 2002; 30:1772–1777

33. Ciesla DJ, Moore EE, Johnson JL, et al.: The role of the lung in postinjury multiple organ failure. *Surgery* 2005; 138:749–757

34. Groven S, Eken T, Skaga NO, et al.: Long-lasting performance improvement after formalization of a dedicated trauma service. *J Trauma* 2011; 70:569–574

35. Sauaia A, Moore EE, Johnson JL, et al.: Temporal trends of postinjury multiple-organ failure: Still resource intensive, morbid, and lethal. *J Trauma Acute Care Surg* 2014; 76:582–592

36. Matthews JN, Altman DG, Campbell MJ, et al.: Analysis of serial measurements in medical research. *BMJ* 1990; 300:230–235

37. Xiao W, Mindrinos MN, Seok J, et al.: A genomic storm in critically injured humans. *J Exp Med* 2011; 208:2581–2590

38. Farrah T, Deutsch EW, Omenn GS, et al.: A high-confidence human plasma proteome reference set with estimated concentrations in PeptideAtlas. *Mol Cell Proteomics* 2011; 10:M110.006353

39. Schiraldi M, Raucci A, Muñoz LM, et al.: HMGB1 promotes recruitment of inflammatory cells to damaged tissues by forming a complex with CXCL12 and signaling via CXCR4. *J Exp Med* 2012; 209:551–563

40. Jones JM, Skaga NO, Søvik S, et al.: Norwegian survival prediction model in trauma: modelling effects of anatomic injury, acute physiology, age, and co-morbidity. *Acta Anaesthesiol Scand* 2014; 58:303–315

41. Evankovich J, Cho SW, Zhang R, et al.: High mobility group box 1 release from hepatocytes during ischemia and reperfusion injury is mediated by decreased histone deacetylase activity. *J Biol Chem* 2010; 285:39888–39897

42. Tsung A, Klune JR, Zhang X, et al.: HMGB1 release induced by liver ischemia involves Toll-like receptor 4 dependent reactive oxygen species production and calcium-mediated signaling. *J Exp Med* 2007; 204:2913–2923

43. Angus DC, Yang L, Kong L, et al.: Circulating high-mobility group box 1 (HMGB1) concentrations are elevated in both uncomplicated pneumonia and pneumonia with severe sepsis. *Crit Care Med* 2007; 35:1061–1067

44. Valdés-Ferrer SI, Rosas-Ballina M, Olofsson PS, et al.: HMGB1 mediates splenomegaly and expansion of splenic CD11b+ Ly-6C(high) inflammatory monocytes in murine sepsis survivors. *J Intern Med* 2013; 274:381–390

45. Martin-Murphy BV, Holt MP, Ju C: The role of damage associated molecular pattern molecules in acetaminophen-induced liver injury in mice. *Toxicol Lett* 2010; 192:387–394

46. Shah N, Montes de Oca M, Jover-Cobos M, et al.: Role of toll-like receptor 4 in mediating multiorgan dysfunction in mice with acetaminophen induced acute liver failure. *Liver Transpl* 2013; 19:751–761

47. Dragomir A-C, Laskin JD, Laskin DL: Macrophage activation by factors released from acetaminophen-injured hepatocytes: potential role of HMGB1. *Toxicol Appl Pharmacol* 2011; 253:170–177

48. Ekong U, Zeng S, Dun H, et al.: Blockade of the receptor for advanced glycation end products attenuates acetaminophen-induced hepatotoxicity in mice. *J Gastroenterol Hepatol* 2006; 21:682–688

49. Okuma Y, Liu K, Wake H, et al.: Anti-high mobility group box-1 antibody therapy for traumatic brain injury. *Ann Neurol* 2012; 72:373–384

50. Cho W, Koo JY, Park Y, et al.: Treatment of sepsis pathogenesis with high mobility group box protein 1-regulating anti-inflammatory agents. *J Med Chem* 2017; 60:170–179

Figure Legends

Figure 1. HMGB1 concentrations during the first 24 h after injury in the 136 patients, shown as a function of elapsed time from injury. Line breakpoints correspond to individual blood samples with concentration measurements. Inset shows HMGB1 concentration decay rates from the first to the second in-hospital samples with regression line and 95% confidence limits for the estimated slope (shaded). The single highest admission value (223 ng/mL) is marked with an asterisk here and in Figs. 2 and 3.

Figure 2. HMGB1 concentrations in 15 example patients during the first 24 h after injury (upper panel), with computed first order decay curves (middle panel) and residual curves (lower panel) generated by subtraction of the first order decay curves from the measured HMGB1 concentrations. Note that this approach forced all residual curves to start at 0 ng/mL. The patients were selected to represent a broad range of HMGB1 concentrations and waveform shapes, corresponding to a broad range of injuries and physiological derangement. Individual patients have the same color across all panels. All concentrations are ng/mL; dashed vertical lines are at 3 and 6 h after injury (cf. Fig. 3, lower rows). *A single admission value of 223 ng/mL is not shown. $^{+}$A single value of 74 ng/mL at 3:50 h after injury is not shown.

Figure 3. HMGB1 concentrations during the first 12 h after injury in the 127 individual patients with documented admission base excess. Upper rows show measured HMGB1 concentrations, middle rows show computed HMGB1 concentrations assuming first order decay kinetics after admission, and lower rows show residual curves obtained by subtracting computed decay curves from measured concentrations (cf. Fig. 2). The curves are grouped by anatomical injury (NISS, New Injury Severity Score; increasing severity from left to right) and physiological derangement (BE, admission base excess in mmol/L). Dashed vertical lines at 3 and 6 h after injury delineate the period used for calculation of second wave $AUC_{3\text{-}6}$. Individual patients have the same color across all panels. *A single value of 223 ng/mL on admission is not shown; this patient was omitted from multivariable outcome analyses including admission HMGB1 because of major influence on results. $^{+}$This patient was omitted from multivariable analyses of outcome because of a particularly large second wave $AUC_{3\text{-}6}$ with major influence on results.

Supplemental Digital Content

Supplemental Digital Content 1. Supplemental Methods. pdf

Supplemental Digital Content 2. Patient inclusion in the study and in individual analyses. pdf

Supplemental Digital Content 3. Supplemental Tables. pdf

TABLE 1. Characteristics of the Study Population

Characteristics	Trauma Patients (*n* = 136)	Healthy Controls (*n* = 20)
Demographics		
Sex (male : female)	101 : 35	11 : 9
Age (years)	40 (27 – 54; 18 – 94); 135	39 (32 – 49; 22 – 58); 20
Pre-injury ASA PS (ASA I : II : III)	85 : 37 : 14	
Injuries		
Mechanism of injury (blunt : penetrating)	118 : 18	
NISS	27 (12 – 47; 1 – 75); 136	
ISS	19 (9 – 34; 1 – 75); 136	
Serious injury (NISS ≥ 16; ISS ≥ 16)	92; 80	
Critical injury (NISS ≥ 25; ISS ≥ 25)	75; 57	
Major head trauma[A] (y : n)	59 : 77	
Abdominal trauma[B] (y : n)	38 : 98	
Admission BE (mmol/L)	-3.1 (-6.1 – -1.3; -26.0 – 3.4); 127	
Admission BE ≤ -6 mmol/L (n)	32	
HMGB1 analyses		
Admission HMGB1 (ng/mL)	3.74 (2.05 – 9.90; 0.31 – 223); 135	0.69 (0.58 – 0.88; 0.41 – 1.35); 20
Second wave AUC_{3-6}[C] (ng/mL×h)	3.15 (1.20 – 5.48; -1.12 – 149); 94	
Time from injury to first sample (hours)	1:15 (0:47 – 1:50; 0:20 – 5:40); 136	
Samples analysed for HMGB1 per patient	6 (5 – 10; 1 – 35); 136	
Hospital treatment		
Hospital length of stay (days)	6 (3 – 13; 1 – 52); 136	
ICU length of stay (days)	3 (2 – 7; 1 – 52); 131	
Ventilator treatment (y : n)	67 : 69	
Survival		
Dead at 30 days (y : n)	20 : 116	
Time to death (days)	1 (0 – 1; 0 – 23); 20	
Predefined outcome variables		
Ventilator-free days	29 (5 – 30; 0 – 30); 136	
Patient weight adjusted total noradrenaline dose 8–48 h after admission (mg/kg)	0 (0 – 99; 0 – 1,101); 136	
Maximal creatinine concentration within 48 h after injury (μmol/L)	84 (72 – 98; 43 – 306); 136	
Maximal ALT concentration within 48 h after injury (U/L)	39 (21 – 88; 8 – 2,356); 135	

Maximal AST concentration within 48 h after injury (U/L)	50 (31 – 106; 17 – 6,085); 111
Maximal bilirubin concentration within 48 h after injury (μmol/L)	11 (7 – 17; 2 – 57); 136

Numbers are given as median (quartiles; range) and number of patients if not otherwise specified.

ASA PS, American Society of Anesthesiologists Physical Status Classification System; NISS, New Injury Severity Score; ISS, Injury Severity Score; BE, Base Excess; ICU, intensive care unit; ALT, alanine aminotransferase; AST, aspartate aminotransferase.

[A]Major head trauma, maximum Abbreviated Injury Scale (AIS) severity code ≥3 in ISS region Head or neck. [B]Abdominal trauma, any AIS code in ISS region Abdominal or pelvic contents. [C]Criteria for inclusion of patients in analyses involving second wave AUC_{3-6} are given in Supplemental Methods (Supplemental Digital Content 1).

TABLE 2. Multivariable Linear Regression Analyses with Admission HMGB1 and Second Wave $AUC_{3–6}$

	Predictors						
	HMGB1		Patient		Injury		
Response	Admission (ng/mL)	Second wave $AUC_{3–6}$ (ng/mL×h)	Sex Male	Age (years)	NISS	BE (mmol/L)	Total Model
HMGB1							
Admission (ng/mL)	–	–	NS	NS	0.64 (0.40 – 0.88) [0.574] p <0.0001	NS	R^2 = 0.24; n = 91; p <0.0001
Second wave $AUC_{3–6}$ (ng/mL×h)	0.17 (0.10 – 0.23) [0.426] p <0.0001	–	NS	NS	NS	-1.28 (-1.56 – -0.99) [0.574] p <0.0001	R^2 = 0.63; n = 85; p <0.0001
Intensive care							
Ventilator-free days	NS	-0.97 (-1.08 – -0.86) [0.868] p <0.0001	NS	-0.05 (-0.09 – 0.00) [0.132] p = 0.06	NS	NS	R^2 = 0.88; n = 50; p <0.0001
Patient weight adjusted total noradrenaline dose 8–48 h after admission (mg/kg)	NS	13.9 (10.8 – 17.0) p <0.0001	NS	NS	NS	NS	R^2 = 0.62; n = 51; p <0.0001
Routine lab; maximal concentrations within 48 h after injury							
Creatinine (μmol/L)	NS	1.05 (0.44 – 1.65) [0.390] p = 0.0009	29 (17 – 41) [0.183] p <0.0001	0.58 (0.31 – 0.85) [0.249] p <0.0001	NS	-1.29 (-2.54 – -0.03) [0.334] p = 0.04	R^2 = 0.50; n = 85; p <0.0001
ALT (U/L)	NS	4.05 (1.66 – 6.45) p = 0.001	NS	NS	NS	NS	R^2 = 0.15; n = 66; p = 0.001
AST (U/L)	NS	8.17 (4.38 – 12.0) p <0.0001	NS	NS	NS	NS	R^2 = 0.27; n = 53; p <0.0001

Only significant values are shown (NS, not significant). Mechanism of injury was not a significant predictor variable for any response, and the response variable Maximal bilirubin concentration within 48 h after injury did not have any significant predictor. Numbers represent effect size with 95% confidence interval in parentheses. In models with more than one significant predictor variable, importance indices in brackets reflect the relative contributions of the individual predictors to the response variable.

Second wave $AUC_{3–6}$, area under the residual curve 3–6 hours after injury; NISS, New Injury Severity Score; BE, Base Excess; ALT, alanine aminotransferase; AST, aspartate aminotransferase. p, significance probability; n, number of patients with complete data contributing to the model; R^2, coefficient of multiple determination, estimating the proportion of variation in the response that can be attributed to the model rather than to random error.

A single patient with an extreme outlier admission HMGB1 concentration (marked with an asterisk in Fig. 1–3) and a single patient with an extreme outlier second wave $AUC_{3–6}$ value (marked with a cross in Fig. 2 and 3) were excluded due to substantial influence on linear regression analyses. Criteria for inclusion of patients in analyses involving second wave $AUC_{3–6}$ are given in Supplemental Methods (Supplemental Digital Content 1), and explanations for the number of patients contributing to each model are given in Supplemental Digital Content 2.

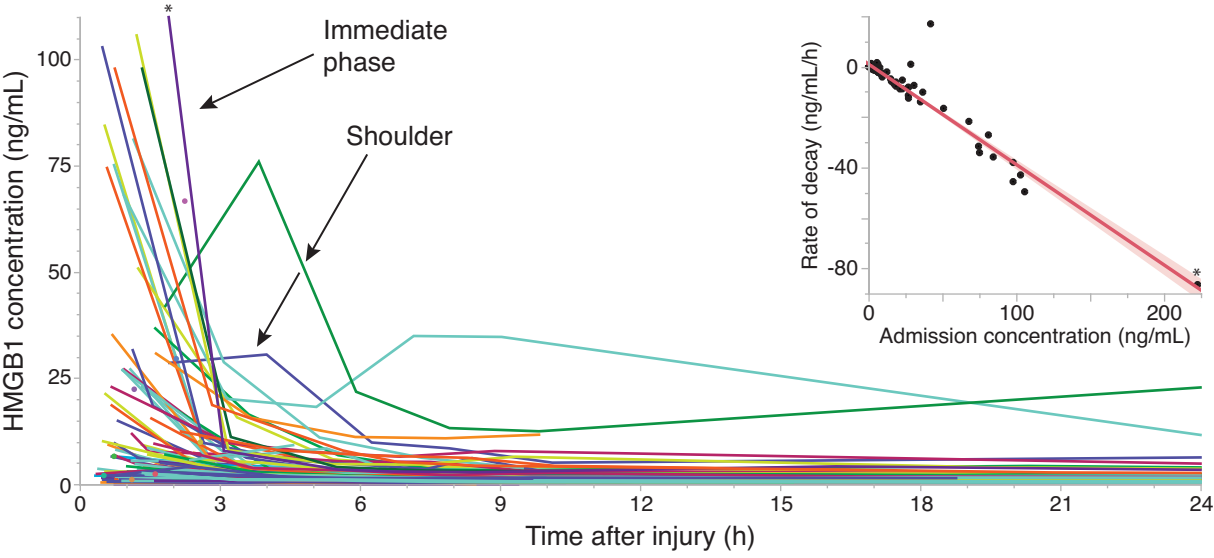
Immediate phase
Shoulder
HMGB1 concentration (ng/mL)
100
75
50
25
0
0
3
6
9
12
15
18
21
24
Time after injury (h)
Rate of decay (ng/mL/h)
0
-40
-80
0
100
200
Admission concentration (ng/mL)

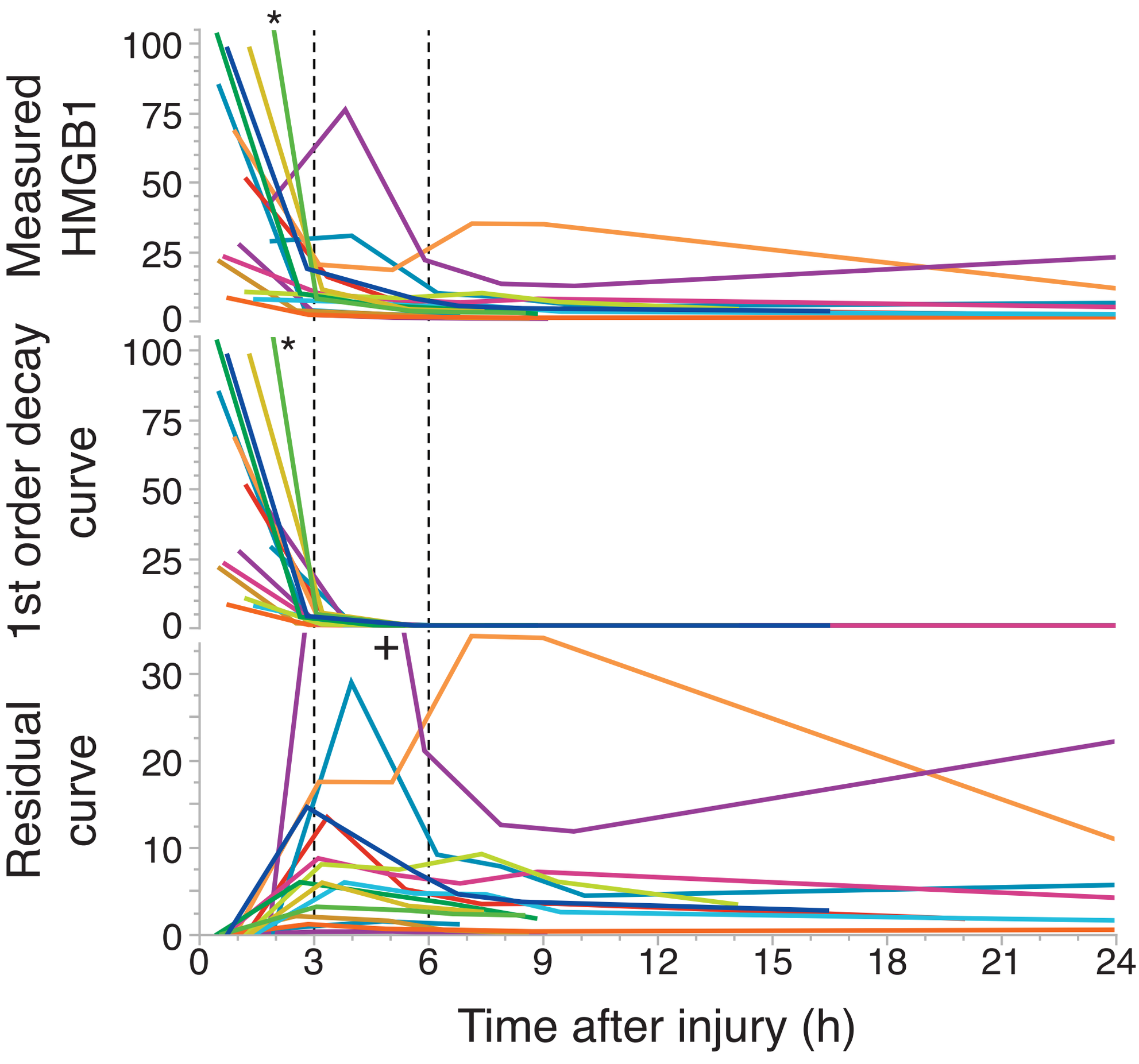
Measured HMGB1
1st order decay curve
Residual curve
*
*
+
100
75
50
25
0
100
75
50
25
0
30
20
10
0
0
3
6
9
12
15
18
21
24
Time after injury (h)

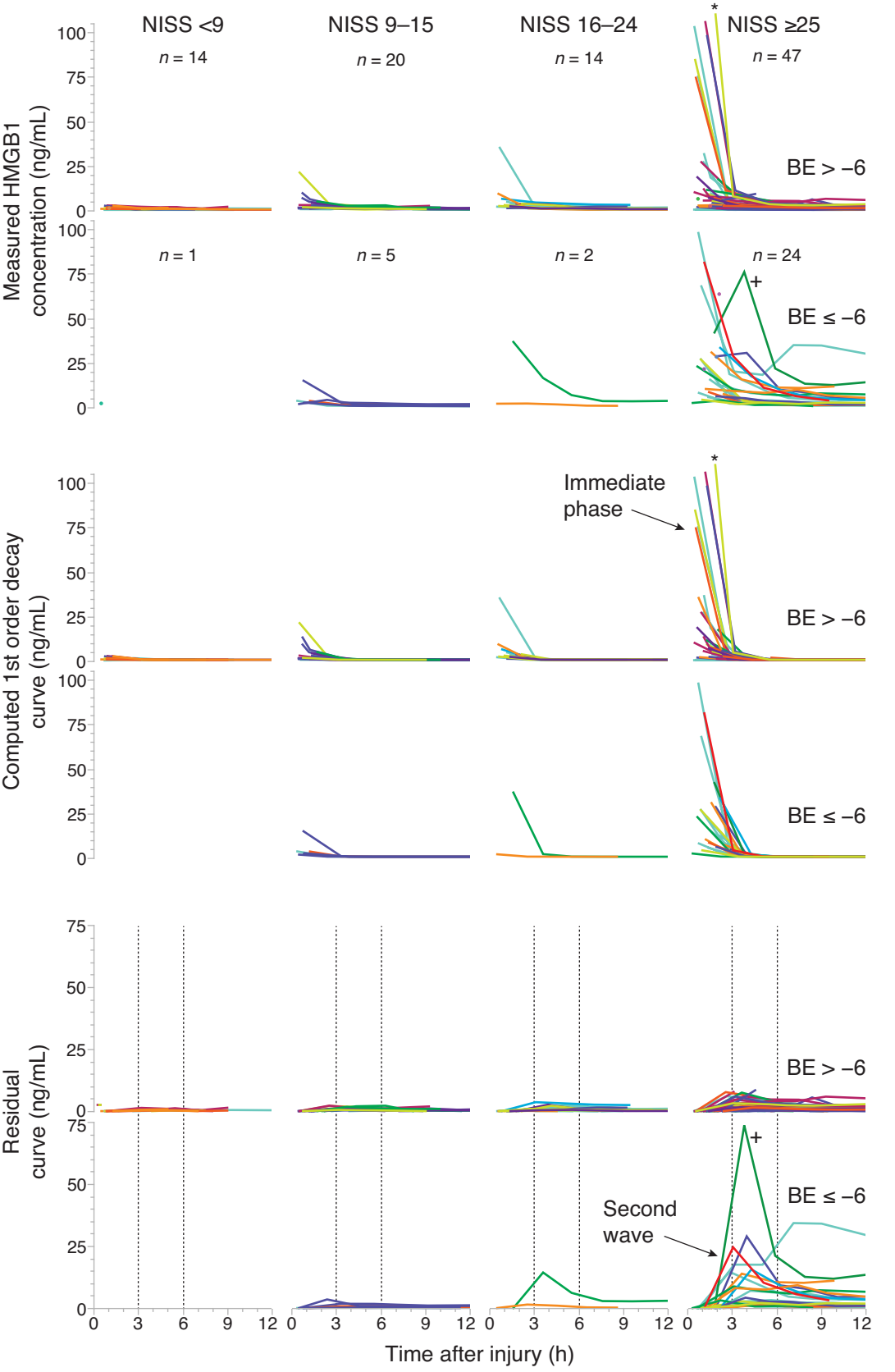
NISS <9
NISS 9–15
NISS 16–24
NISS ≥25
n = 14
n = 20
n = 14
n = 47
n = 1
n = 5
n = 2
n = 24
BE > −6
BE ≤ −6
Measured HMGB1 concentration (ng/mL)
Computed 1st order decay curve (ng/mL)
Residual curve (ng/mL)
Immediate phase
Second wave
Time after injury (h)
0
3
6
9
12
25
50
75
100

Supplemental Methods

Analysis of Repeated HMGB1 Measurements

A first order kinetic curve was fitted to the measured HMGB1 concentrations for the patient population (concentration above baseline $C(t) = C_0 \times e^{-kt}$, where C_0 was admission HMGB1 concentration above baseline, t was time after the admission sample was obtained). Baseline was defined as median HMGB1 concentration from the control group, 0.69 ng/mL, see Table 1 and Supplemental Table 1 (Supplemental Digital Content 3) which describe the study population. Only values from the first two time points after admission in patients with clearly elevated admission HMGB1 concentrations, arbitrarily defined as ≥3 ng/mL, were used. The elimination rate constant (k) was estimated using successive approximation to find the lowest value that did not yield any negative values in the residual curves (cf. Fig. 3, lower rows). Half-life was calculated as $t_{1/2} = \ln(2)/k$.

The estimated elimination rate constant was used together with each patient's actual baseline-adjusted HMGB1 concentration at admission, to compute individual concentration decay curves above baseline (0.69 ng/mL, see above) for all individual patients. The individual computed concentration decay curves were subtracted from the actual measured HMGB1 concentrations, to obtain individual residual curves.

Except for HMGB1 concentration at admission, all measured and computed HMGB1 concentrations were analyzed as function of elapsed time after injury. The temporally aligned concentration curves were linearly interpolated with 7.5 min time resolution to enable analyses mandating comparison at specific times after injury across our asynchronously sampled data. The linearly interpolated data set was also utilized to calculate area under the individual HMGB1 concentration curves as a function of time, using the trapezoidal rule. The application for linear interpolation followed by integration was custom developed in LabVIEW 2013 (National Instruments, Austin, TX).

Quantitative relationships with residual curve HMGB1 concentration over time were investigated using area under the residual curves from 3 to 6 h after injury (second wave $AUC_{3–6}$, always analyzed as a continuous variable), because this time period contained the most prominent part of the second waves (see Fig. 3, lower rows). Only patients with admission samples obtained no later than 2 h after injury were included, in order to minimize the effect of forcing all admission residual concentrations to zero (Fig. 3, lower rows). Additionally, all patients who had missing samples between 2 and 7 hours after injury were omitted, including those who were dead or discharged up to 7 h after injury. Detailed explanations for the number of patients contributing to comparisons and models are given in Supplemental Digital Content 2.

STROBE flow diagram for patient inclusion and blood samples analyzed for HMGB1

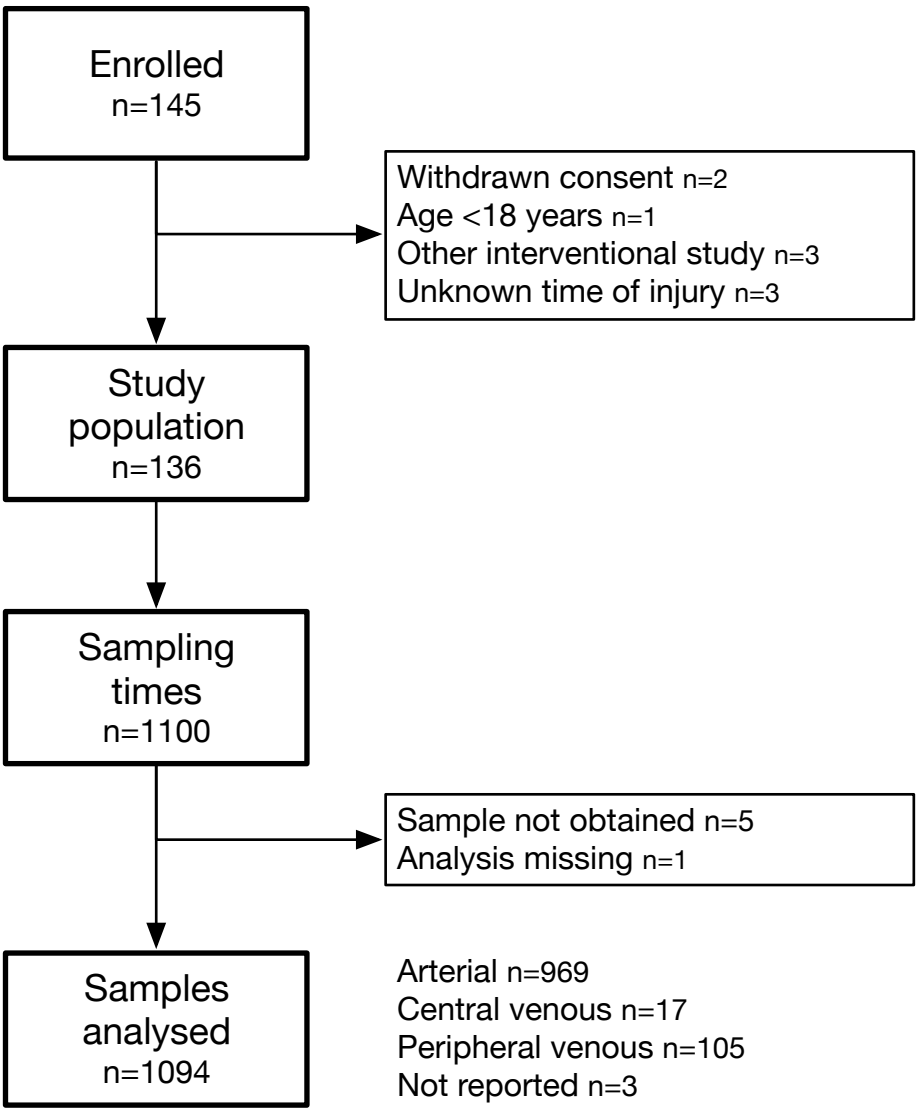

Flow diagram for the 136 study participants and 1094 samples analyzed for HMGB1, according to von Elm E, Altman DG, Egger M et al.: The Strengthening the Reporting of Observational Studies in Epidemiology (STROBE) statement: Guidelines for reporting observational studies. *Lancet* 2007; 370:1453–1457.

Number of HMGB1 analyses per time code and per patient

The blood sampling scheme was highly consistent. Samples were obtained from five patients during helicopter transfer to our trauma center (T00), and from all 136 patients at admission (coded as T01; 135 HMGB1 analyses due to one analysis missing, cf. STROBE flow diagram above). Samples were then collected every two hours after T01 until eight hours after admission (T05), followed by every morning in the ICU and/or postoperative care unit until a maximum of 10 days after injury (T15). Six pilot patients were followed throughout their ICU stay.

The following figure shows number of patients with HMGB1 analyses at each of our defined sampling time codes. Note that time codes were converted to elapsed time from time of injury (defined as zero hours) in all analyses of concentration kinetics:

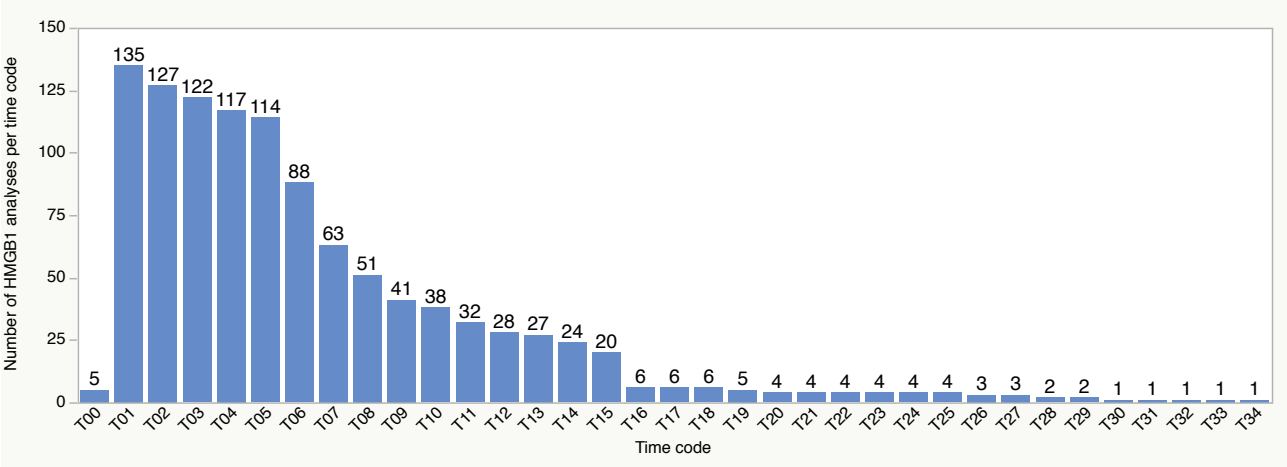

As a consequence of the sampling acquisition scheme, the number of HMGB1 analyses *per patient* varied from 1 to 35 (median 6, quartiles 5–10). This is illustrated in the following figure:

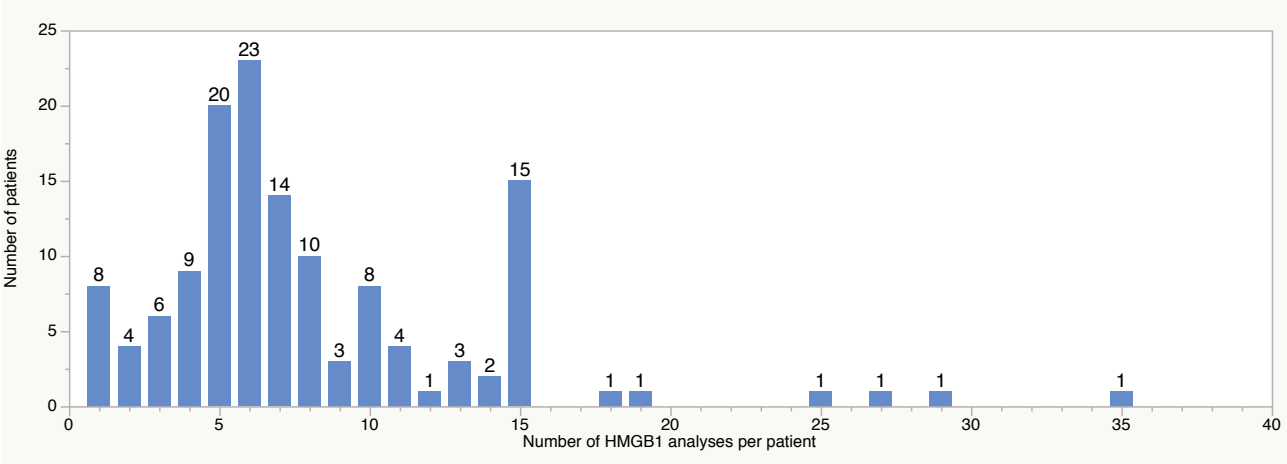

Number of patients in the individual statistical analyses

Distribution of the 136 study participants between the categories utilized for statistical analyses is outlined in the Venn diagram below:

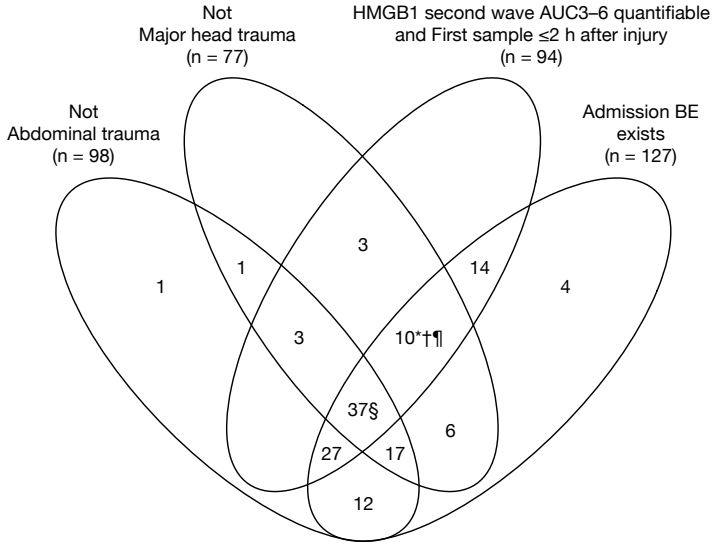

The diagram includes the following four patients (only one attribute per patient):

§ A patient without information about Age

¶ A patient without analysis of Admission HMGB1

* A patient with exceptionally high Admission HMGB1 (marked with an asterisk in Figs. 1–3) was excluded from the models in Table 2 and in Supplemental Tables 2–4 (Supplemental Digital Content 3) due to substantial influence on linear regression analyses

† A patient with exceptionally high Second wave $AUC_{3–6}$ (marked with a cross in Figs. 2–3) was excluded from the models in Table 2 and in Supplemental Tables 2–4 (Supplemental Digital Content 3) due to substantial influence on linear regression analyses

One single patient with combined abdominal and head trauma, no valid HMGB1 second wave $AUC_{3–6}$, and no admission BE (i.e., outside the four ovals) is not shown in any diagram.

Colored areas (intersections) in the following Venn diagrams highlight patients meeting all criteria for the respective analyses.

Table 2: Multivariable linear regression analyses with Admission HMGB1 and Second wave $AUC_{3–6}$

Explanations for the number of patients included in the final linear regression model for each response variable in Table 2 are given below.

All analyses were restricted to the 94 patients with quantifiable Second wave $AUC_{3–6}$ (who had their first sample taken within 2 h after injury (colored area in the first Venn diagram below; see Supplemental Methods, Supplemental Digital Content 1). Added constraints when patients with abdominal trauma or major head trauma were excluded from the analysis, and when admission BE or age was a significant predictor, are visualized as colored intersections in the following Venn diagrams.

Admission HMGB1: 94 patients with Second wave $AUC_{3–6}$ (colored area below), 1 excluded due to missing Admission HMGB1 (¶), 1 due to exceptionally high Admission HMGB1 (*), and 1 due to exceptionally high Second wave $AUC_{3–6}$ (†), n = 91

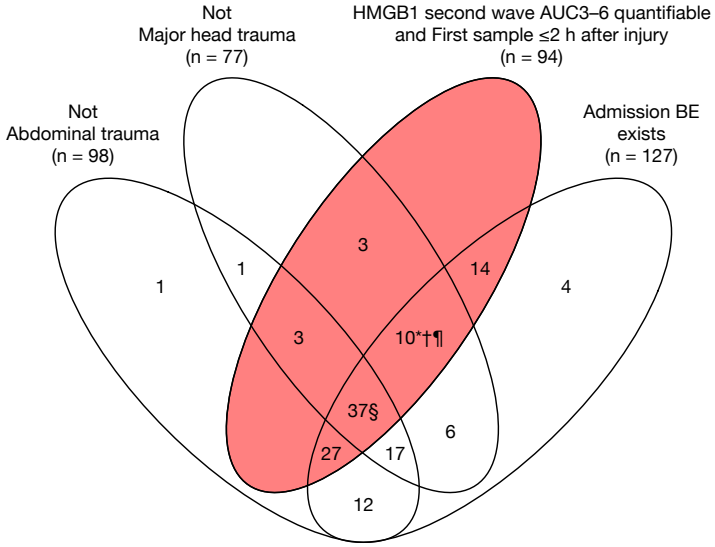

Second wave $AUC_{3–6}$: 88 patients with Second wave $AUC_{3–6}$ and BE (colored area below), 1 excluded due to missing Admission HMGB1 (¶), 1 due to exceptionally high Admission HMGB1 (*), and 1 due to exceptionally high Second wave $AUC_{3–6}$ (†), n = 85

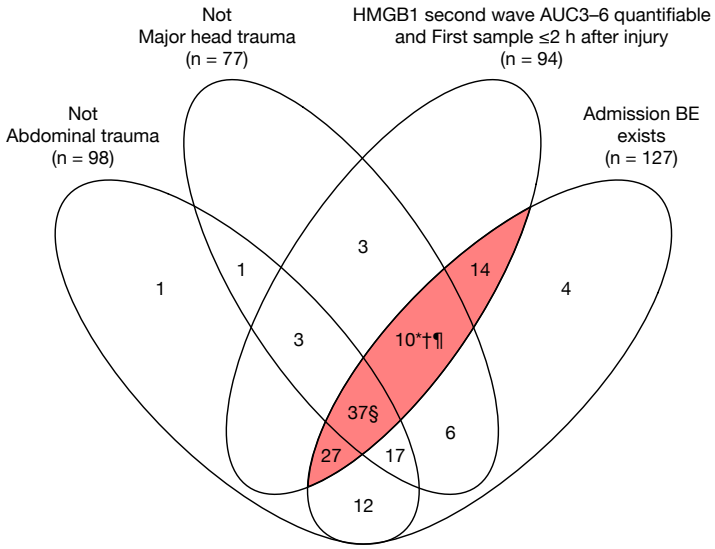

Ventilator-free days: 53 patients with Second wave $AUC_{3–6}$ and without Major head trauma (colored area below), 1 excluded due to exceptionally high Admission HMGB1 (*), 1 due to exceptionally high Second wave $AUC_{3–6}$ (†), and 1 due to missing Age (§), n = 50

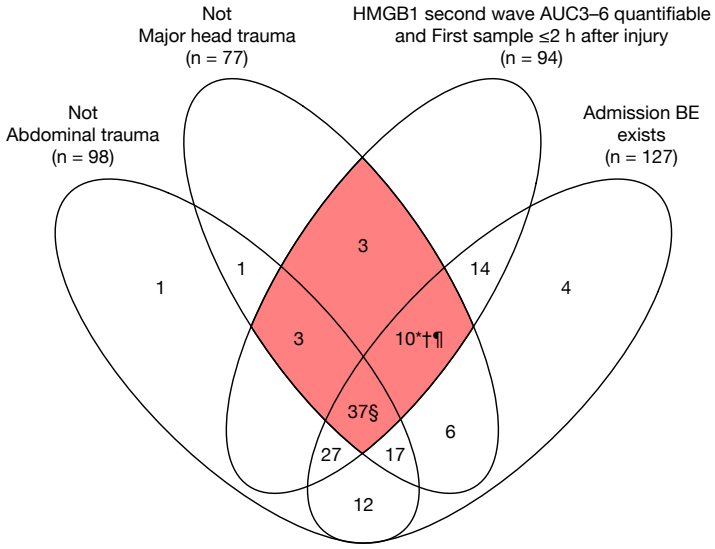

Patient weight adjusted total noradrenaline dose: 53 patients with Second wave $AUC_{3–6}$ and without Major head trauma (colored area above), 1 excluded due to exceptionally high Admission HMGB1 (*) and 1 due to exceptionally high Second wave $AUC_{3–6}$ (†), n = 51

Creatinine: 88 patients with Second wave $AUC_{3–6}$ and admission BE (colored area below), 1 excluded due to exceptionally high Admission HMGB1 (*), 1 due to exceptionally high Second wave $AUC_{3–6}$ (†), and one due to missing Age (§), n = 85

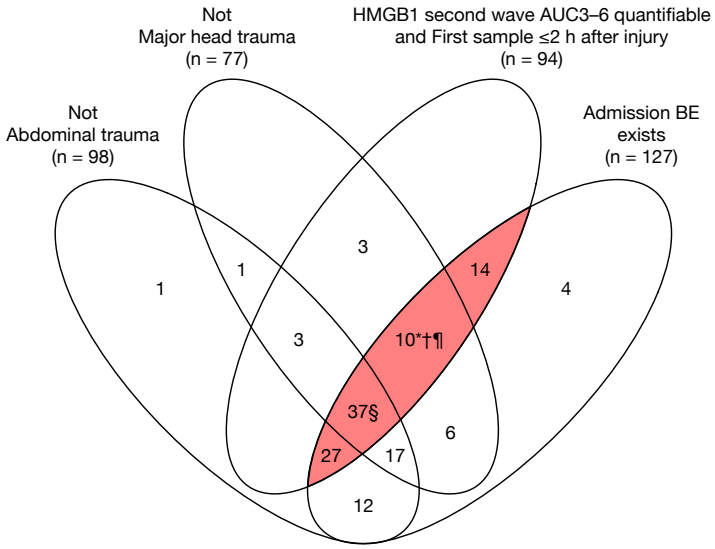

ALT: 67 patients with Second wave $AUC_{3–6}$ and without abdominal trauma (colored area below), 1 excluded due to missing ALT analysis, n = 66

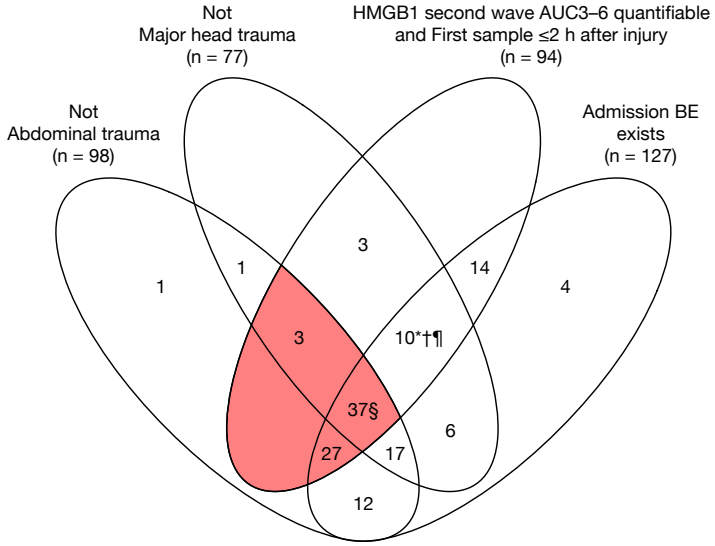

AST: 67 patients with Second wave $AUC_{3–6}$ and without abdominal trauma (colored area above), 14 excluded due to missing AST analysis, n = 53

Supplemental Tables 2 and 3: Bivariable correlations among the 136 patients

Maximum number of patients available for analyses with Admission HMGB1: 136 patients in total population, 1 excluded due to missing Admission HMGB1 (¶), 1 due to exceptionally high Admission HMGB1 (*), n = 134

Maximum number of patients available for analyses with Second wave $AUC_{3–6}$: 94 patients (colored area below), 1 excluded due to exceptionally high Second wave $AUC_{3–6}$ (†), n = 93

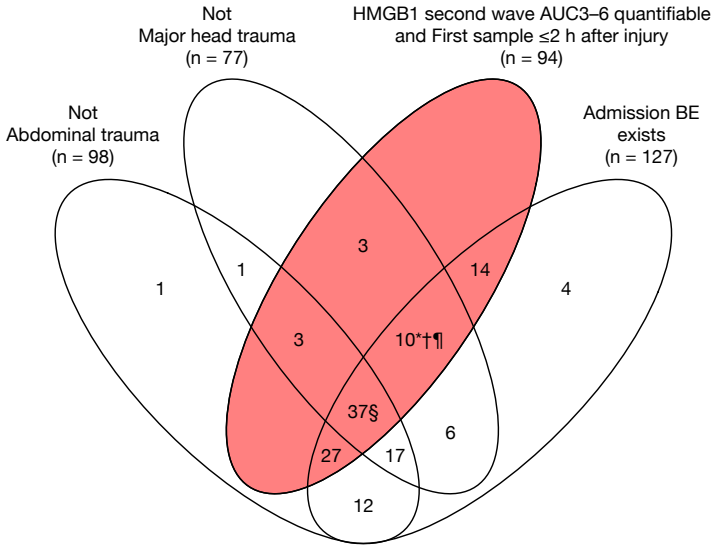

Supplemental Table 4: Multivariable linear regression analyses with Admission HMGB1

Explanation for the number of patients included in the final linear regression model for each response variables in Supplemental Table 4 is given below.

As for Supplemental Tables 2 and 3, the maximum number of patients available for analyses with Admission HMGB1 was 134: 136 patients in the total population, 1 excluded due to missing Admission HMGB1 (¶) and 1 due to exceptionally high Admission HMGB1 (*). No patient was excluded from analyses due to missing information about sex or NISS. Added constraints are described and visualized.

Admission HMGB1: 127 patients with Admission BE (colored area below), 1 excluded due to missing Admission HMGB1 (¶) and 1 due to exceptionally high Admission HMGB1 (*), n = 125

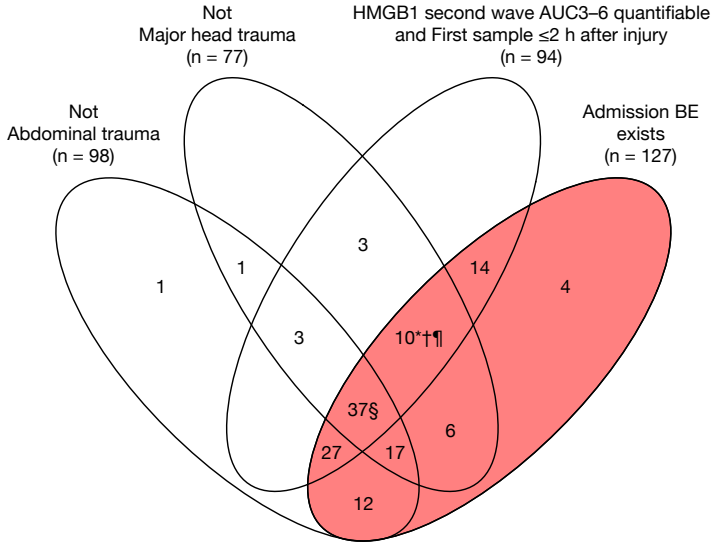

Ventilator-free days: 70 patients with Admission BE and without Major head trauma (colored area below), 1 excluded due to exceptionally high Admission HMGB1 (*), n = 69

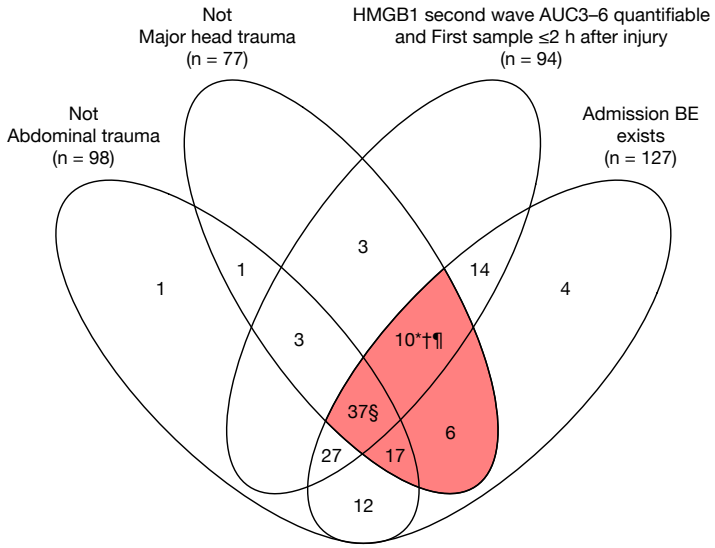

Patient weight adjusted total noradrenaline dose: 77 patients without Major head trauma (colored area below), 1 excluded due to exceptionally high Admission HMGB1 (*), n = 76

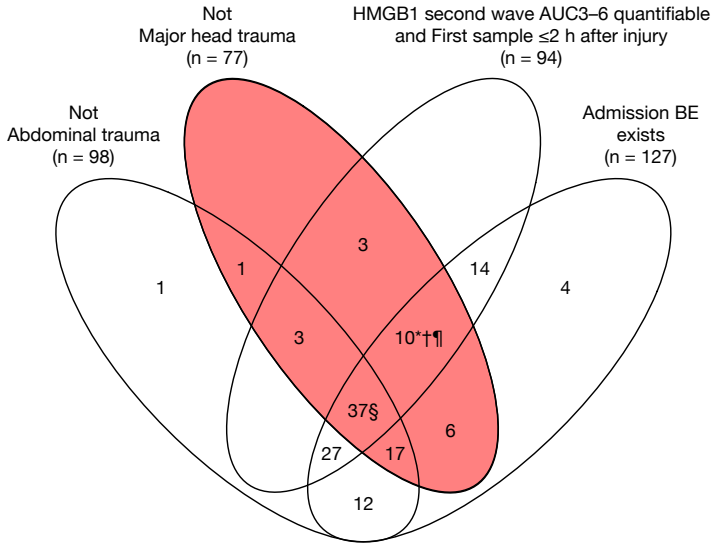

Creatinine: 127 patients with Admission BE (colored area below), 1 excluded due to exceptionally high Admission HMGB1 (*) and 1 due to missing Age (§), n = 125

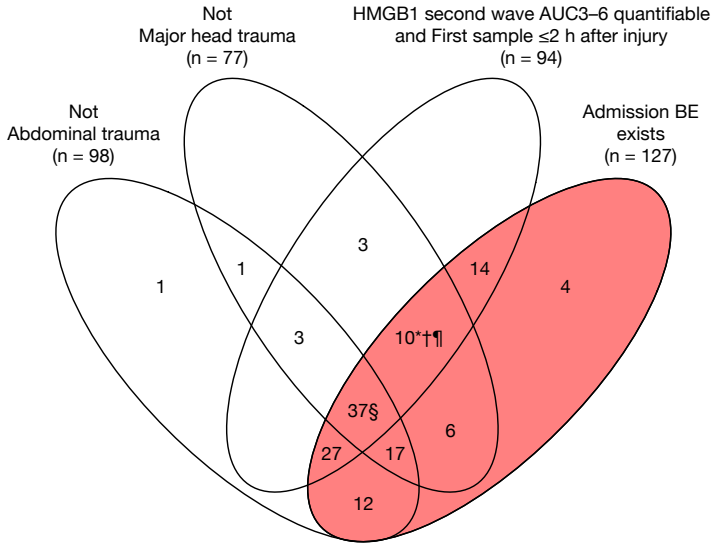

ALT: 98 patients without Abdominal trauma (colored area below), 1 excluded due to missing ALT analysis, n = 97

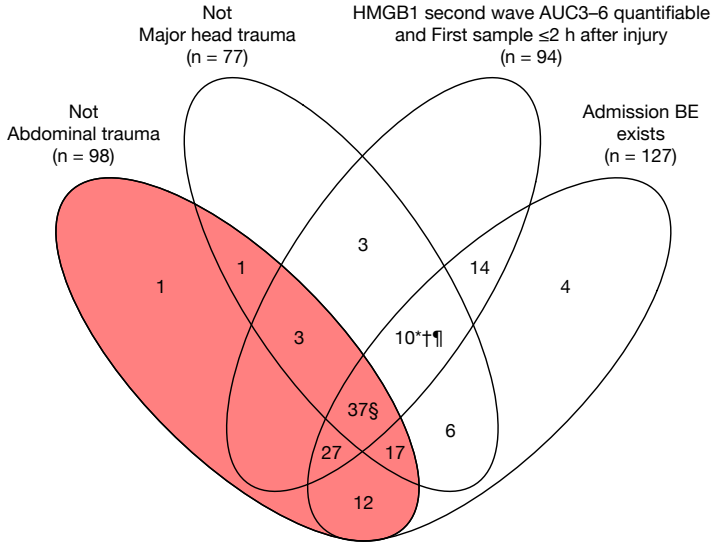

AST: 93 patients with Admission BE and without Abdominal trauma (colored area below), 18 excluded due to missing AST analyses, n = 75

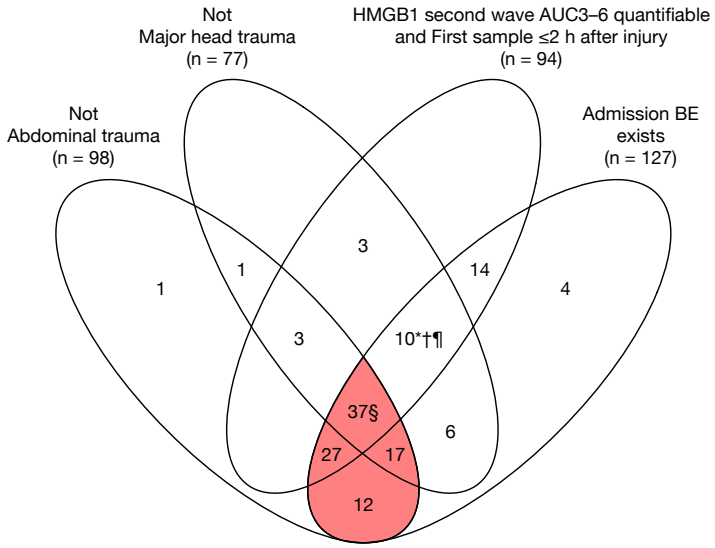

SUPPLEMENTAL TABLE 1. Detailed Characteristics of the Study Population

Characteristics	All Trauma Patients (n = 136)	Major Head Trauma		p	Abdominal Trauma		p	Healthy Controls (n = 20)
		Yes (n = 59)	No (n = 77)		Yes (n = 38)	No (n = 98)		
Demographics								
Sex (male : female)	101 : 35	44 : 15	57 : 20	1.00	28 : 10	73 : 25	1.00	11 : 9
Age (years)	40 (27 – 54; 18 – 94); 135	42 (26 – 63; 18 – 94); 59	37 (28 – 50; 18 – 75); 76	0.17	37 (26 – 54; 18 – 89); 38	40 (28 – 53; 18 – 94); 97	0.86	39 (32 – 49; 22 – 58); 20
Pre-injury ASA PS (ASA I : II : III)	85 : 37 : 14	31 : 19 : 9	54 : 18 : 5	0.08	25 : 9 : 4	60 : 28 : 10	0.85	
Injuries								
Mechanism of injury (blunt : penetrating)	118 : 18	52 : 7	66 : 11	0.80	36 : 2	82 : 16	0.10	
NISS	27 (12 – 47; 1 – 75); 136	48 (34 – 57; 10 – 75); 59	14 (9 – 27; 1 – 59); 77	<0.0001	42 (27 – 57; 9 – 66); 38	22 (10 – 41; 1 – 75); 98	0.0001	
ISS	19 (9 – 34; 1 – 75); 136	34 (26 – 43; 9 – 75); 59	10 (6 – 19; 1 – 43); 77	<0.0001	34 (24 – 43; 4 – 66); 38	13 (9 – 26; 1 – 75); 98	<0.0001	
Admission BE (mmol/L)	-3.1 (-6.1 – -1.3; -26.0 – 3.4); 127	-3.9 (-6.3 – -1.5; -26.0 – 2.1); 57	-3.0 (-5.1 – -1.1; -25.9 – 3.4); 70	0.25	-4.8 (-9.4 – -1.7; -26.0 – 2.1); 34	-2.9 (-4.7 – -1.2; -22.8 – 3.4); 93	0.02	
HMGB1 analyses								
Admission HMGB1 (ng/mL)	3.74 (2.05 – 9.90; 0.31 – 223); 135	4.88 (2.08 – 22.4; 0.45 – 106); 59	3.01 (1.84 – 7.52; 0.31 – 223); 76	0.12	23.0 (6.78 – 67.3; 0.71 – 223); 37	2.62 (1.72 – 5.43; 0.31 – 103); 98	<0.0001	0.69 (0.58 – 0.88; 0.41 – 1.35); 20
Second wave $AUC_{3–6}$[A] (ng/mL×h)	3.15 (1.20 – 5.48; -1.12 – 149); 94	3.75 (2.02 – 9.91; -0.82 – 62.2); 41	2.79 (0.91 – 4.90; -1.12 – 149); 53	0.07	5.94 (3.12 – 26.4; 0.00 – 149); 27	2.31 (0.91 – 4.70; -1.12 – 29.8); 67	0.0002	
Time from injury to first sample (hours)	1:15 (0:47 – 1:50; 0:20 – 5:40); 136	1:23 (0:55 – 2:00; 0:28 – 5:40); 59	1:07 (0:44 – 1:35; 0:20 – 4:06); 77	0.02	1:18 (0:44 – 1:51; 0:32 – 3:43); 38	1:15 (0:47 – 1:46; 0:20 – 5:40); 98	0.83	
Time from admission to first sample (hours)	0:10 (0:06 – 0:16; 0:00 – 1:27); 136	0:10 (0:05 – 0:16; 0:00 – 1:27); 59	0:10 (0:06 – 0:16; 0:00 – 0:53); 77	0.63	0:10 (0:06 – 0:18; 0:00 – 1:20); 38	0:10 (0:06 – 0:15; 0:00 – 1:27); 98	0.25	
Samples analysed for HMGB1 per patient	6 (5 – 10; 1 – 35); 136	8 (5 – 15; 1 – 29); 59	6 (4 – 7; 1 – 35); 77	<0.0001	7 (5 – 12; 1 – 29); 38	6 (5 – 10; 1 – 35); 98	0.37	
Hospital treatment								
Primary : secondary admission	120 : 16	47 : 12	73 : 4	0.01	34 : 4	86 : 12	1.00	
Time from injury to admission (hours)	0:58 (0:37 – 1:28; 0:10 – 5:25); 136	1:05 (0:44 – 1:35; 0:13 – 5:25); 59	0:52 (0:35 – 1:22; 0:10 – 3:50); 77	0.06	0:59 (0:36 – 1:28; 0:17 – 2:45); 38	0:58 (0:38 – 1:30; 0:10 – 5:25); 98	0.97	
Hospital length of stay (days)	6 (3 – 13; 1 – 52); 136	8 (3 – 15; 1 – 52); 59	5 (3 – 11; 1 – 50); 77	0.02	7 (2 – 16; 1 – 52); 38	6 (3 – 12; 1 – 50); 98	0.97	
ICU length of stay (days)	3 (2 – 7; 1 – 52); 131	6 (2 – 14; 1 – 52); 57	2 (2 – 5; 1 – 35); 74	0.0008	4 (2 – 10; 1 – 52); 35	3 (2 – 7; 1 – 35); 96	0.45	
Ventilator treatment (y : n)	67 : 69	47 : 12	20 : 57	<0.0001	22 : 16	45 : 53	0.25	
Time on a ventilator (days)	3 (2 – 15; 1 – 35); 67	6 (2 – 15; 1 – 35); 47	2 (1 – 9; 1 – 26); 20	0.07	3 (2 – 18; 1 – 35); 22	6 (2 – 13; 1 – 22); 45	0.99	
Transferred to other hospital while still intubated (y : n)	25 : 42	22 : 25	3 : 17	0.02	11 : 11	14 : 31	0.18	
Survival								
Dead at 30 days (y : n)	20 : 116	16 : 43	4 : 73	0.0005	11 : 27	9 : 89	0.006	
Time to death (days)	1 (0 – 1; 0 – 23); 20	1 (0 – 1; 0 – 23); 16	0 (0 – 2; 0 – 3); 4	0.31	0 (0 – 1; 0 – 23); 11	1 (1 – 6; 0 – 12); 9	0.08	
Predefined outcome variables								
Ventilator-free days	29 (5 – 30; 0 – 30); 136	9 (0 – 28; 0 – 30); 59	30 (29 – 30; 0 – 30); 77	<0.0001	12 (0 – 30; 0 – 30); 38	30 (15 – 30; 0 – 30); 98	0.004	
Patient weight adjusted total noradrenaline dose 8–48 h after admission (mg/kg)	0 (0 – 99; 0 – 1,101); 136	23 (0 – 411; 0 – 1,101); 59	0 (0 – 0; 0 – 870); 77	<0.0001	0 (0 – 278; 0 – 870); 38	0 (0 – 73; 0 – 1,101); 98	0.25	
Maximal creatinine concentration within 48 h after injury (μmol/L)	84 (72 – 98; 43 – 306); 136	83 (72 – 112; 48 – 166); 59	84 (72 – 97; 43 – 306); 77	0.56	85 (73 – 113; 63 – 306); 38	84 (71 – 97; 43 – 210); 98	0.31	
Maximal ALT concentration within 48 h after injury (U/L)	39 (21 – 88; 8 – 2,356); 135	40 (23 – 95; 8 – 936); 58	38 (21 – 86; 8 – 2,356); 77	0.64	92 (44 – 327; 8 – 2,356); 38	32 (20 – 53; 8 – 287); 97	<0.0001	
Maximal AST concentration within 48 h after injury (U/L)	50 (31 – 106; 17 – 6,085); 111	61 (36 – 117; 21 – 1,528); 50	47 (28 – 99; 17 – 6,085); 61	0.11	131 (66 – 426; 28 – 6,085); 32	38 (27 – 65; 17 – 415); 79	<0.0001	
Maximal bilirubin concentration within 48 h after injury (μmol/L)	11 (7 – 17; 2 – 57); 136	12 (8 – 17; 2 – 47); 59	10 (7 – 17; 2 – 57); 77	0.12	13 (7 – 21; 2 – 47); 38	10 (7 – 16; 2 – 57); 98	0.09	

Numbers are given as median (quartiles; range) and number of patients if not otherwise specified. Major head trauma was defined as maximum Abbreviated Injury Scale (AIS) severity code ≥3 in Injury Severity Score (ISS) region Head or neck, and Abdominal trauma as any AIS code in ISS region Abdominal or pelvic contents. ASA PS, American Society of Anesthesiologists Physical Status Classification System; NISS, New Injury Severity Score; ISS, Injury Severity Score; BE, Base Excess; ICU, intensive care unit; ALT, alanine aminotransferase; AST, aspartate aminotransferase. p values represent two-tailed probability for group comparisons with Fisher's exact test for categorical data and Wilcoxon rank-sum test with correction for ties for continuous data. [A]Criteria for inclusion of patients in analyses involving second wave $AUC_{3–6}$ are given in Supplemental Methods (Supplemental Digital Content 1), see also Supplemental Digital Content 2.

SUPPLEMENTAL TABLE 2. Bivariable Analyses, Non-Parametric Correlations

	HMGB1												BE (mmol/L)								
	Admission[A] (ng/mL)			Second Wave $AUC_{3–6}$[B] (ng/mL×h)			Age (years)			NISS			Total Population			Blunt Injury			Penetrating Injury		
	ρ	*n*	*p*	ρ	*n*	*p*	ρ	*n*	*p*	ρ	*n*	*p*	ρ	*n*	*p*	ρ	*n*	*p*	ρ	*n*	*p*
HMGB1																					
Admission[A] (ng/mL)	-	-	-	0.71	91	<0.0001	-0.01	133	0.92	0.49	134	<0.0001	-0.43	125	<0.0001	-0.47	108	<0.0001	-0.67	17	0.003
Second wave $AUC_{3–6}$[B] (ng/mL×h)	0.71	91	<0.0001	-	-	-	-0.17	92	0.10	0.54	93	<0.0001	-0.50	87	<0.0001	-0.59	74	<0.0001	-0.28	13	0.35
Ventilator-free days																					
Total population	-0.42	134	<0.0001	-0.51	93	<0.0001	-0.12	135	0.18	-0.75	136	<0.0001	0.46	127	<0.0001	0.46	110	<0.0001	0.40	17	0.11
Not Major head trauma	-0.36	75	0.002	-0.44	52	0.001	-0.03	76	0.80	-0.45	77	<0.0001	0.41	70	0.0004	0.36	60	0.005	0.49	10	0.15
Major head trauma	-0.40	59	0.002	-0.46	41	0.003	-0.04	59	0.75	-0.71	59	<0.0001	0.45	57	0.0005	0.52	50	0.0001	0.09	7	0.85
Patient weight adjusted total noradrenaline dose 8–48 h after admission (mg/kg)																					
Total population	0.24	134	0.005	0.40	93	<0.0001	0.03	135	0.69	0.57	136	<0.0001	-0.33	127	0.0002	-0.35	110	0.0002	-0.27	17	0.30
Not Major head trauma	0.29	75	0.01	0.36	52	0.009	0.10	76	0.40	0.48	77	<0.0001	-0.29	70	0.02	-0.35	60	0.007	0.06	10	0.87
Major head trauma	0.07	59	0.58	0.28	41	0.08	-0.09	59	0.48	0.30	59	0.02	-0.29	57	0.03	-0.25	50	0.08	-0.56	7	0.20
Routine lab; maximal concentrations within 48 h after injury																					
Creatinine (μmol/L)	0.31	134	0.0003	0.34	93	0.0008	0.17	135	0.04	0.22	136	0.01	-0.28	127	0.001	-0.27	110	0.004	-0.24	17	0.36
ALT (U/L)	0.57	133	<0.0001	0.42	92	<0.0001	-0.07	134	0.41	0.24	135	0.006	-0.25	126	0.005	-0.37	109	<0.0001	-0.07	17	0.78
AST (U/L)	0.65	110	<0.0001	0.57	76	<0.0001	0.004	111	0.97	0.42	111	<0.0001	-0.30	103	0.002	-0.47	86	<0.0001	0.12	17	0.64
Bilirubin (μmol/L)	0.12	134	0.12	0.39	93	0.0001	-0.21	135	0.02	0.23	136	0.007	-0.02	127	0.80	-0.01	110	0.92	-0.25	17	0.34

ρ, Spearman's rank correlation coefficient; *n*, number of patients; *p*, significance probability for ρ. Major head trauma was defined as maximum Abbreviated Injury Scale (AIS) severity code ≥3 in Injury Severity Score (ISS) region Head or neck.

Second wave $AUC_{3–6}$, area under the residual curve 3–6 hours after injury; NISS, New Injury Severity Score; BE, Base Excess; ALT, alanine aminotransferase; AST, aspartate aminotransferase.

Criteria for inclusion of patients in analyses involving second wave $AUC_{3–6}$ are given in Supplemental Methods (Supplemental Digital Content 1), and explanation for the number of patients contributing to the analyses are given in Supplemental Digital Content 2. [A]A single patient with an extreme outlier admission HMGB1 concentration (marked with an asterisk in Fig. 1–3) was excluded due to substantial influence on linear regression analyses. [B]The single patient with an extreme outlier value (marked with a cross in Fig. 2 and 3) was excluded due to substantial influence on linear regression analyses.

SUPPLEMENTAL TABLE 3. Bivariable Analyses, Group Comparisons

	Sex			Mechanism of Injury		
	Male	Female	*p*	Blunt	Penetrating	*p*
HMGB1						
Admission[A] (ng/mL)	3.75 (2.22 – 10.1; 0.31 – 106); 99	2.40 (1.29 – 7.42; 0.45 – 98); 35	0.11	4.32 (2.07 – 14.3; 0.31 – 106); 116	2.47 (1.43 – 4.41; 0.67 – 29); 18	0.04
Second wave $AUC_{3–6}$[B] (ng/mL×h)	3.18 (1.28 – 5.48; -1.12 – 62); 74	2.54 (1.19 – 4.91; -0.82 – 56); 19	0.74	3.24 (1.20 – 6.03; -1.12 – 56); 79	2.10 (0.99 – 3.66; -0.29 – 62); 14	0.18
Ventilator-free days						
Total population	30 (4 – 30; 0 – 30); 101	28 (4 – 30; 0 – 30); 35	0.30	29.5 (0 – 30; 0 – 30); 118	28.5 (11 – 30: 0 – 30); 18	0.69
Not Major head trauma	30 (30 – 30; 0 – 30); 57	30 (28 – 30; 0 – 30); 20	0.10	30 (29 – 30; 0 – 30); 66	30 (28 – 30; 0 – 30); 11	0.34
Major head trauma	9 (0 – 29; 0 – 30); 44	9 (0 – 24; 0 – 30); 15	0.95	8.5 (0 – 29; 0 – 30); 52	12 (0 – 28; 0 – 29); 7	0.79
Patient weight adjusted total noradrenaline dose 8–48 h after admission (mg/kg)						
Total population	0 (0 – 15; 0 – 1,101); 101	7.2 (0 – 411; 0 – 1,096); 35	0.004	0 (0 – 101; 0 – 1,101); 118	0 (0 – 125; 0 – 950); 18	0.85
Not Major head trauma	0 (0 – 0; 0 – 500); 57	0 (0 – 26; 0 – 870); 20	0.04	0 (0 – 0; 0 – 870); 66	0 (0 – 0; 0 – 67); 11	0.49
Major head trauma	0 (0 – 268; 0 – 1,101); 44	409 (10 – 607; 0 – 1,096); 15	0.01	16 (0 – 403; 0 – 1,101); 52	297 (0 – 813; 0 – 950); 7	0.37
Routine lab; maximal concentrations within 48 h after injury						
Creatinine (μmol/L)	89 (78 – 102; 43 – 210); 101	71 (59 – 79; 44 – 306); 35	<0.0001	84 (72 – 97; 43 – 306); 118	91 (72 – 104; 50 – 151); 18	0.45
ALT (U/L)	40 (23 – 86; 8 – 1,137); 100	34 (17 – 105; 8 – 2,356); 35	0.37	42 (25 – 95; 8 – 2,356); 117	22 (13 – 32; 8 – 582); 18	0.002
AST (U/L)	50 (32 – 96; 17 – 2,755); 81	49 (25 – 179; 19 – 6,085); 30	0.80	58 (33 – 131; 19 – 6,085); 94	28 (26 – 45; 17 – 837); 17	0.003
Bilirubin (μmol/L)	12 (8 – 18; 2 – 57); 101	8 (6 – 14; 2 – 47); 35	0.07	10 (8 – 16; 2 – 57); 118	12 (6 – 19; 2 – 30); 18	0.94

Numbers represent median (quartiles; range) and number of patients. *p*, probability for group comparisons with Wilcoxon rank-sum test. Major head trauma was defined as maximum Abbreviated Injury Scale (AIS) severity code ≥3 in Injury Severity Score (ISS) region Head or neck.

Second wave $AUC_{3–6}$, area under the residual curve 3–6 hours after injury; NISS, New Injury Severity Score; BE, Base Excess; ALT, alanine aminotransferase; AST, aspartate aminotransferase.

Criteria for inclusion of patients in analyses involving second wave $AUC_{3–6}$ are given in Supplemental Methods (Supplemental Digital Content 1), and explanation for the number of patients contributing to the analyses are given in Supplemental Digital Content 2. [A]A single patient with an extreme outlier admission HMGB1 concentration (marked with an asterisk in Fig. 1–3) was excluded due to substantial influence on linear regression analyses. [B]The single patient with an extreme outlier value (marked with a cross in Fig. 2 and 3) was excluded due to substantial influence on linear regression analyses.

SUPPLEMENTAL TABLE 4. Multivariable Linear Regression Analyses with Admission HMGB1

	Predictors					
	HMGB1	Patient		Injury		
Response	Admission (ng/mL)	Sex Male	Age (years)	NISS	BE (mmol/L)	Total Model
HMGB1						
Admission (ng/mL)	–	NS	NS	0.42 (0.22 – 0.61) [0.613] p <0.0001	-0.83 (-1.54 – -0.13) [0.387] p = 0.02	R^2 = 0.21; n = 125; p <0.0001
Intensive care						
Ventilator-free days	NS	NS	NS	-0.23 (-0.35 – -0.12) [0.399] p = 0.0001	0.79 (0.51 – 1.07) [0.601] p <0.0001	R^2 = 0.55; n = 69; p <0.0001
Patient weight adjusted total noradrenaline dose 8–48 h after admission (mg/kg)	NS	NS	NS	5.12 (3.06 – 7.19) p <0.0001	NS	R^2 = 0.25; n = 76; p <0.0001
Routine lab; maximal concentrations within 48 h after injury						
Creatinine (μmol/L)	NS	20 (8 – 32) [0.218] p = 0.002	0.31 (0.01 – 0.61) [0.187] p = 0.04	0.33 (0.03 – 0.63) [0.335] p = 0.03	-1.83 (-2.88 – -0.79) [0.476] p = 0.0007	R^2 = 0.24; n = 125; p <0.0001
ALT (U/L)	1.34 (0.48 – 2.19) p = 0.003	NS	NS	NS	NS	R^2 = 0.09; n = 97; p = 0.003
AST (U/L)	1.38 (0.06 – 2.69) [0.537] p = 0.04	NS	NS	NS	-3.70 (-7.56 – 0.15) [0.463] p = 0.06	R^2 = 0.13; n = 75; p = 0.007

Only significant values are shown (NS, not significant). Mechanism of injury was not a significant predictor variables for any response, and the response variable Maximal bilirubin concentration within 48 h after injury did not have any significant predictor. Numbers represent effect size with 95% confidence interval in parentheses. In models with more than one significant predictor variable, importance indices in brackets reflect the relative contributions of the individual predictors to the response variable.

NISS, New Injury Severity Score; BE, Base Excess; ALT, alanine aminotransferase; AST, aspartate aminotransferase. p, significance probability; n, number of patients with complete data contributing to the model; R^2, coefficient of multiple determination, estimating the proportion of variation in the response that can be attributed to the model rather than to random error.

A single patient with an extreme outlier admission HMGB1 concentration (marked with an asterisk in Fig. 1–3) was excluded due to substantial influence on linear regression analyses. Explanations for the number of patients contributing to each model are given in Supplemental Digital Content 2.